Short Communications

Contributions intended for publication under this heading should be expressly so marked; they should not exceed about 500 words; they should be forwarded in the usual way to the appropriate Co-editor; they will be published as speedily as possible; and proofs will not generally be submitted to authors. Publication will be quicker if the contributions are without illustrations.

Acta Cryst. (1955). **8**, 510

On the superstructure of the alloy Cu_3Pd.

By D. Watanabe, M. Hirabayashi and S. Ogawa, *The Research Institute for Iron, Steel and other Metals, Tôhoku University, Sendai, Japan*

(Received 28 March 1955 and in revised form 21 April 1955)

The Cu–Pd alloy Cu_3Pd has been investigated by Jones & Sykes (1939) and by Jones & Owen (1954). It was shown that at temperatures above about 460° C. Cu_3Pd has a disordered face-centred cubic lattice, whereas the slowly cooled alloy is in the ordered state and has a face-centred tetragonal lattice (α'' phase) in which the arrangement of atoms is different from that in Cu_3Au but of which the detailed structure was not known. If, however, the ordered structure be considered in terms of the disordered face-centred cell then, as the cooling proceeded, it was found that the axial ratio c/a diminishes from unity for the disordered state to 0·985 below about 270° C.

We have studied the structure of the α'' phase of Cu–Pd alloys in thin orientated films by electron diffraction and in single crystals by X-rays.

Fig. 1(*a*) shows an electron-diffraction pattern of a thin alloy film containing 25 atomic % Pd, which was rapidly cooled from 230° C. after slow cooling from 450° C. in several hundred hours. The pattern resembles that of the partially ordered Cu_3Au alloy containing anti-phase domains (Raether, 1952), and more closely that of CuAu II (Ogawa & Watanabe, 1954), but in the present case the splitting of superlattice reflexions is more complex. In order to explain the pattern in Fig. 1(*a*), we consider a complicated two-dimensional anti-phase domain structure as shown in Fig. 2(*a*). This structure can be thought of as formed from the elemental face-centred tetragonal lattice in which the atoms arrange themselves as in the ordered structure of Cu_3Au but in which the two kinds of stepshift, $\pm\frac{1}{2}(\mathbf{a}_1\pm\mathbf{a}_2)$ and $\pm\frac{1}{2}(\mathbf{a}_3\pm\mathbf{a}_1)$, occur at every M_3th atom and M_1th atom along the z and x directions respectively ($\mathbf{a}_1$, $\mathbf{a}_2$ and $\mathbf{a}_3$ are the fundamental lattice vectors in the x, y and z directions respectively). The former type of shift (the first kind of out-of-step) is identical with that in the partially ordered state of Cu_3Au (Guinier & Griffoul, 1948), and that in CuAu II (Johansson & Linde, 1936), but the latter (the second kind of out-of-step) has not so far been found. The two kinds of one-dimensional anti-phase domains, characterized by the two kinds of step-shift, are not independent, but are associated with each other. Thus a two-dimensional anti-phase domain structure is formed and the large unit cell, outlined by the thick lines in Fig. 2(*a*), has an orthorhombic symmetry (the lattice constants are $2M_1a_1$, a_2, and $2M_3a_3$). The tetragonal axis of the elemental tetragonal cell lies along the z direction.

The structure amplitude of this proposed model can easily be calculated, and the intensity distribution in reciprocal space is derived as shown in Fig. 2(*b*). In this figure circles correspond to the intensity weight due to three kinds of two-dimensional anti-phase domain structure, in each of which the tetragonal axis coincides with one of three original cubic axes. It is to be pointed out

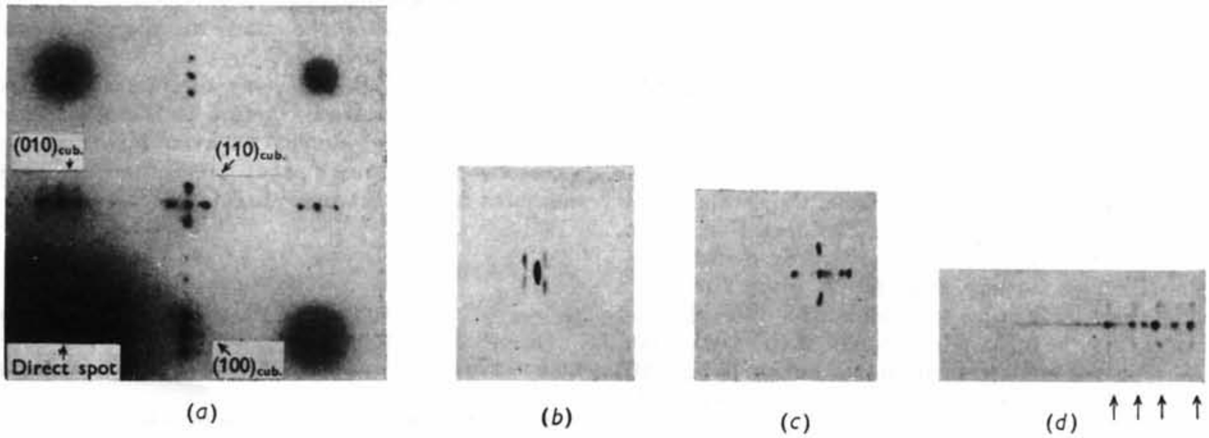

(*a*) (*b*) (*c*) (*d*)

Fig. 1. (*a*) Electron-diffraction pattern of thin alloy film containing 25 atomic % Pd; $\{100\}_{cub.}$ and $\{110\}_{cub.}$ reflexions show complex splitting. Weak spots are also seen between them.

(*b*) Oscillation X-ray photograph of $(112)_{cub.}$ reflexion for the alloy of 22 atomic % Pd; $[110]_{cub.}$ is vertical; unfiltered Fe radiation. Only one kind of separation is seen.

(*c*) Stationary-crystal X-ray photograph of $(210)_{cub.}$ reflexion for the alloy of 27 atomic % Pd; $[001]_{cub.}$ is vertical and $[100]_{cub.}$ is 35° from beam direction; unfiltered Cu radiation. Two kinds of separation are clearly shown.

(*d*) Oscillation X-ray photograph of $(310)_{cub.}$ reflexion for the alloy of 27 atomic % Pd; $[001]_{cub.}$ is vertical; unfiltered Fe radiation. The arrows show the weak splitting spots.

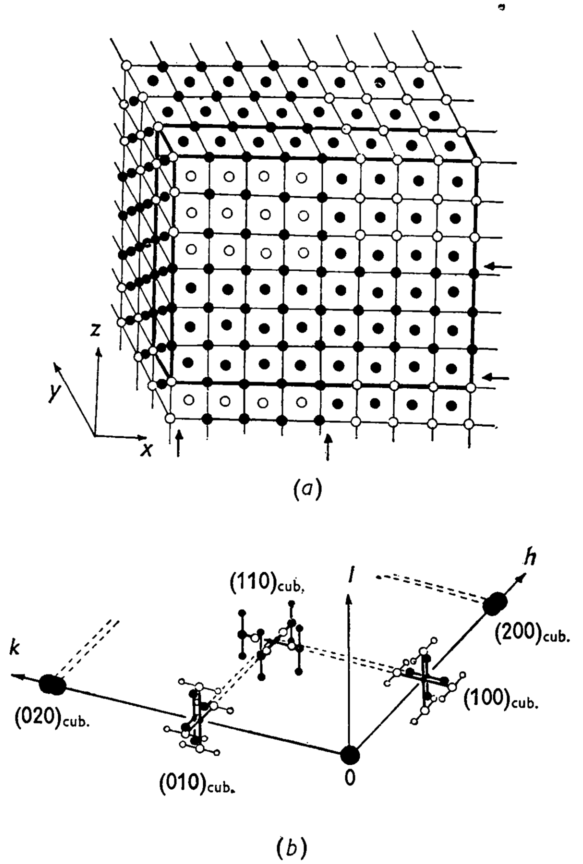

Fig. 2. (*a*) Two-dimensional anti-phase domain structure. Full and open circles represent Cu and Pd atoms respectively. $M_1 = 4$ and $M_3 = 3$ are chosen in this model. Out-of-steps occur at places indicated by arrows.

(*b*) Intensity distribution in reciprocal space. *h*, *k* and *l* refer to the original cubic system. The superlattice reflexions shown by small open circles represent the splitting from the reciprocal-lattice points $(100)_{\text{tet.}}$, $(010)_{\text{tet.}}$ and $(110)_{\text{tet.}}$; full circles represent the splitting from the other lattice points, $(001)_{\text{tet.}}$, $(101)_{\text{tet.}}$ and $(011)_{\text{tet.}}$.

that there are two kinds of separation in the splitting of the superlattice points, corresponding to the values of M_1 and M_3. The pattern in Fig. 1(*a*)* coincides well with the *hk* plane of zero level.

For the X-ray studies, single crystals in the fully ordered states were obtained by slow cooling from 400° C. to 200° C. in four months. We took oscillation photographs and sometimes a series of stationary-crystal photographs, keeping either the [100] or the [110] direction of the original cubic lattice as the vertical axis. Fig. 1(*b*, *c*, *d*) shows some examples of the photographs for two single crystals. For the alloy of 22 atomic% Pd, the splitting of each superlattice reflexion can well be interpreted by assuming the presence of one-dimensional anti-phase domains, characterized by the first kind of out-of-step and lined up along the tetragonal axis with the length $M_3 \simeq 7$. On the other hand, the photographs of the alloy containing 27 atomic% Pd are explained by the intensity distribution in reciprocal space as shown in Fig. 2(*b*), and therefore both kinds of anti-phase domains are confirmed to exist along the *x* and *z* directions with the lengths $M_1 \simeq 4$ and $M_3 \simeq 3$ respectively.

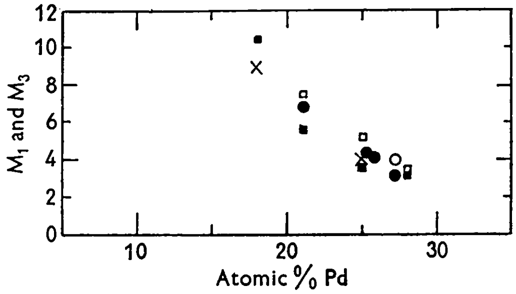

Fig. 3. Variation with composition of the lengths of anti-phase domains. Open and full circles represent the values of M_1 and M_3 obtained by X-ray study, and open and full squares are those obtained by electron-diffraction study respectively. Crosses are the values of M_3 obtained by Schubert *et al.* (1954).

The splitting of superlattice reflexions becomes more distinct with the duration of annealing, as if the observed structure were a stable one for the α″ phase. In Fig. 3 the values of M_1 and M_3, obtained by X-ray as well as electron-diffraction studies, are plotted as a function of composition. They are, in general, not integers and decrease with the increasing concentration of Pd.

Recently some investigators have reported the different results for the superstructure of the α″ phase. Geisler & Newkirk (1954) have concluded from the Debye–Scherrer pattern that the ordered Cu_4Pd alloy possesses a superstructure of the modified Ni_4Mo type, entirely different from that described above. Their model cannot, however, explain the diffraction patterns of single crystals shown in Fig. 1. On the other hand, the powder pattern obtained by them can be explained by the model of one-dimensional anti-phase domains characterized by the first kind of out-of-step as well as by the model of the two-dimensional anti-phase domain structure as mentioned above. Schubert, Kiefer & Wilkens (1954) have reported, also using powder specimens, that the alloys containing 18·5–25 atomic% Pd possess an anti-phase domain structure, which corresponds to the first kind of out-of-step in the present case, and that the ordered alloys containing 25–29 atomic% Pd have a more complicated structure. As shown in Fig. 3, the values of M_3 obtained by them agree well with the present results.

A detailed report will shortly be published elsewhere.

References

Geisler, A. H. & Newkirk, J. B. (1954). *J. Metals, N.Y.* **6**, 1076.

Guinier, A. & Griffoul, R. (1948). *Rev. Métall.* **45**, 387.

Johansson, C. H. & Linde, J. O. (1936). *Ann. Phys., Lpz.* **25**, 1.

Jones, D. M. & Owen, E. A. (1954). *Proc. Phys. Soc.* B, **67**, 297.

---

* In Fig. 1(*a*) satellites are observed around the normal spots, including the direct spot, as in the case of CuAu II (Ogawa & Watanabe, 1954). Their origin seems, however, not to be explained from the present model alone.

Jones, F. W. & Sykes, C. (1939). *J. Inst. Met.* **65**, 419.
Ogawa, S. & Watanabe, D. (1954). *J. Phys. Soc. Japan*, **9**, 475.
Raether, H. (1952). *Z. angew. Phys.* **4**, 53.
Schubert, K., Kiefer, B. & Wilkens, M. (1954). *Z. Naturforsch.* **9a**, 987.

Acta Cryst. (1955). **8**, 512

Photographic intensity scales for use with three-dimensional data.

By H. J. Grenville-Wells,*
Department of Chemical Crystallography, University College, Gower Street, London W.C. 1, *England*

(*Received* 29 *April* 1955)

Measurements of the intensities of X-ray diffraction maxima on higher layer lines, whether on oscillation or Weissenberg photographs, must be corrected for a number of effects. The Lorentz and polarization corrections have now been combined with the Cox–Shaw factor (Cox & Shaw, 1930) in a single chart (Cochran, 1948; Kaan & Cole, 1949) and will not be considered here. This note, which deals specifically with oscillation photographs, is concerned with two aspects of the obliquity correction, which has been discussed by Bullen (1953), Qurashi (1953) and Whittaker (1953). First, oblique incidence alters the shape of the spot and increases its area, thus decreasing the blackening of the spot as ν_n, the inclination of the diffracted beam to the equatorial layer, increases. Secondly, when a film-pack (Robertson, 1943) is used, oblique incidence increases the ratio of the intensities in higher layers recorded on successive films because the path length in the films traversed by the diffracted beams increases as ν_n increases.

If I_0 and I are the intensities of the incident and transmitted beams respectively, μ is the effective absorption coefficient and t the thickness of the film, then the film factor for the nth layer is given by

$$R_n = (I_0/I)_n = \exp(\mu t \sec \nu_n)\,, \quad (1)$$

so that

$$R_0 = (I_0/I)_0 = \exp(\mu t) \quad (2)$$

and

$$\log_e(R_n/R_0) = \mu t\,[\sec \nu_n - 1]\,. \quad (3)$$

(For the double-coated X-ray film now in general use, $\mu t \approx 1$, so that for the nth layer line $R_n \approx \exp(\sec \nu_n)$, and $R_n/R_0 \approx 2{\cdot}7$ for $\nu_n = 60°$, which shows how rapidly the intensity falls off on the highest layers of successive films in a film pack.)

Corrections of this type, though tedious, can be applied numerically. It is, however, a matter of common experience that large errors are liable to arise in the visual estimation of intensities when spots of unequal size and shape are to be compared; the greatest difficulty which in practice attends the measurement of oscillation photographs is the change in size and shape of the spots on higher layers due to oblique incidence.

It is customary to estimate the intensities with a scale prepared by choosing a suitable reflexion on the zero layer and recording a series of increasing exposures of this reflexion on the same film, and then assuming that the reciprocity law holds. This method suggests a very simple experimental technique for dealing with both the problems introduced by oblique incidence.

Suppose an intensity scale is made with a pack of three films, S_1, S_2 and S_3, and an oscillation photograph of the crystal is recorded on a pack of three similar films, C_1, C_2 and C_3. Then (writing S_1 for the intensity of the reflexion *hkl* on the film S_1) we have, for any reflexion on the zero layer,

$$(C_1/S_1)_0 = (C_2/S_2)_0 = (C_3/S_3)_0\,.$$

However, if this zero-layer intensity scale is used to measure intensities on higher layer lines,

$$(C_1)_n/(S_1)_0 > (C_2)_n/(S_2)_0 > (C_3)_n/(S_3)_0\,,$$

and numerical corrections must be applied.

If, however, the complete upper half on an oscillation photograph having a few reflexions on each layer be used to prepare an intensity scale film-pack—as has been done in Fig. 1 by using only one of the two screens on a Weissenberg camera—then scales consisting of spots of the correct sizes and shapes are available for every layer, so that visual comparison is very much easier. Further, since

$$(C_1/S_1)_n = (C_2/S_2)_n = (C_3/S_3)_n\,, \quad (4)$$

the need for numerical corrections to compensate for the increased film factor for higher layers is eliminated.

Although equation (4) shows that the values of R_n are not in fact required when this technique is employed, they can be obtained experimentally from such a multilayer scale, since $R_n = (S_1/S_2)_n = (S_2/S_3)_n$. Some values are given below to indicate the magnitude of the obliquity effect and the accuracy obtained. The observations should satisfy equations (1), (2) and (3); thus if $\log_e R_n$ is plotted against $\sec \nu_n$, a straight line should be obtained whose slope is equal to μt, and thus gives R_0, the customary film factor for X-rays incident normally upon a film-pack. For Ilford 'Industrial G' film the results shown in Table 1 were obtained from the set of scales to which Fig. 1 belongs.

Table 1

				R_n (calc.)	
n	ν_n	$\sec \nu_n$	R_n (obs.)	$\mu t = 1{\cdot}20$	$\mu t = 1{\cdot}15$
0	0	1·00	3·33	3·20	3·05
1	6·6	1·01	3·33	3·35	3·18
2	13·8	1·03	3·33	3·44	3·27
3	20·8	1·07	3·64	3·61	3·42
4	28·4	1·14	4·00	3·92	3·69
5	35·1	1·22	∼4·00	4·34	4·08
6	45·8	1·43	5·00	5·60	5·21
7	57·0	1·84	7·50	9·06	8·25

This gives a value of $R_0 > 3$, a rather high figure which has, nevertheless, been found on several occasions for this film. It can be seen from the values of R_n(calc.) shown in the table that there is an apparent departure

---

* I.C.I. Research Fellow.